An operationally implementable model for predicting the effects of an infectious disease on a comprehensive regional healthcare system

Daniel Chertok[1*], Chad Konchak[1], Nirav Shah[1,2], Kamaljit Singh[1], Loretta Au[1], Jared Hammernik[1], Brian Murray[1], Anthony Solomonides[1], Ernest Wang[1], Lakshmi Halasyamani[1,2]

1 NorthShore University HealthSystem, Evanston, Illinois, United States of America
2 University of Chicago Pritzker School of Medicine, Chicago, Illinois, United States of America

* dchertok@northshore.org

Abstract

An operationally implementable predictive model has been developed to forecast the number of COVID-19 infections in the patient population, hospital floor and ICU censuses, ventilator and related supply chain demand. The model is intended for clinical, operational, financial and supply chain leaders and executives of a comprehensive healthcare system responsible for making decisions that depend on epidemiological contingencies. This paper describes the model that was implemented at NorthShore University HealthSystem and is applicable to any communicable disease whose risk of reinfection for the duration of the pandemic is negligible.

Introduction

Upon its emergence in 2020, the COVID-19 pandemic presented immediate challenges to the operation of NorthShore University HealthSystem, a comprehensive regional healthcare system located in the northern part of Chicago, IL, and its suburbs. The need to forecast the expected demand on floor and ICU beds, ventilators and requisite supplies became pressing at the onset of the disease. The lack of reliable population data posed additional difficulty in implementing a usable model. Additional constraints of robustness, distributability and transparency imposed further requirements on the choice of the governing equations, solution algorithm and software implementation. During the initial stage of the pandemic, the model was delivered to the operational stakeholders daily; as time progressed, the frequency of dissemination was changed to once or twice a week, depending on the severity of the situation.

At the onset of the pandemic, the Clinical Analytics team was tasked with providing a reliable, scalable solution relevant to the local epidemiological situation [6]. While abundant literature exists on the theoretical aspects of the problem [1] – [5], [10] – [20], few specific worked examples that could be used by practitioners for immediate implementation are widely available[1]. While most of the existing publications that offer applicable practical solutions focus on country-wide statistics [25], those dealing with local conditions are scarce. In order to find a satisfactory answer to this challenge, we had to quickly construct a flexible, scalable model easily adaptable to rapidly changing

[1]For a concise but comprehensive description of challenges facing a researcher attempting to develop a workable model see, e.g., [27]

conditions that could be quickly communicated to a growing number of stakeholders while affording them an opportunity to create area-specific "back-of-an-envelope" analyses suitable for their needs. This task was accomplished by augmenting the industry-standard SIR model [1] with bootstrapping estimates and interpolation and extrapolation approximations of patient flow dynamics. The resulting model was robust enough to exhibit accuracy sufficient for predicting floor, general intensive care unit (ICU), ventilator census and mortality up to two weeks in advance. The main accomplishments of the foregoing approach were the ability to quickly adapt the model to the observed coefficient of transmission (R_0) prevalent in the hospital service area, compute the forward expected length of stay on the hospital floor, in the ICU and on the ventilator, and incorporate actual and projected vaccination rates into the model.

The paper is organized as follows. First, we review generally accepted modeling principles for forecasting the progression of the disease (COVID-19). Next, we provide empirical formulas for approximating dynamically observed rates of hospitalizations, ICU and ventilator placement, mortality and vaccination. Following that, we present the results and discuss their accuracy. We conclude with a summary of findings and directions for further research.

Materials and methods

General equations

The most widely accepted practical approach to modeling the spread of a highly infectious communicable disease is the Susceptible-Infected-Recovered (SIR) model [1], [2] with a time-dependent coefficient of transmission [3] and vaccination effects. From the practical standpoint, the need to develop a workable model prior to the publication of [3], as well as the need to have a robust, distributable software solution, necessitated the adoption of a simplified time-dependent form[1]

$$dS(t) = -(\beta(t)S(t)I(t) + V(t))dt \,, \tag{1}$$
$$dI(t) = (\beta(t)S(t) - \gamma)I(t)dt \,, \tag{2}$$

where

$S(t)$ - fraction of the population susceptible to the disease,

$I(t)$ - fraction of the population currently infected with the disease,

$\beta(t)$ - coefficient of transmission,

$V(t)$ - fraction of the population that has been vaccinated,

γ - fraction of the infected population removed from further consideration due to (permanent) recovery or death.

We are not concerned with the dynamics of the recovered population, and hence leave the "R" term out of Eq. (1 - 2). Since the dynamics for $\beta(t)$ and $V(t)$ are not known beforehand, they are not included in the differential equations as separate terms, and are instead left to be determined at a later discretization stage. For simplicity, we disregarded mobility considerations reviewed in [24] and [28].

[1] Note that the time dependency of β precludes the use of an analytical solution described in [4].

Numerical solution

Data extrapolation and scenario analysis

At the onset of the pandemic, there is no reliable way to determine the true number of infected patients and hence the transmission coefficient $\beta(t)$. While initial attempts were made to infer likely epidemiological dynamic from countries where the initial stage had by that time already passed [5], the validity of this approach was questionable even at that time since different locales exhibited different curve characteristics. In view of this, the approach adopted for the purpose of constructing a robust model applicable to local conditions was as follows:

1. assume that the number of observed NorthShore (NS) cases reflected the actual count of the disease in the population[1];
2. extrapolate the evolution of $\beta(t)$ implied by the historical data[2];
3. repeat 1 - 2 for the Chicago / Cook / Lake county (CCL) area containing the majority of the NS catchment area;
4. construct a dynamic (time-dependent) ratio of NS to CCL cases and assume that it accurately reflects the proportion of CCL patients attributable to NS;
5. solve Eq. (1 - 2) separately for CCL and NS;
6. use the minimum and maximum case number estimates from step 5 as boundaries for the expected number of NS cases.

Specifically, for step 2, we need to find the value of $\beta(t)$ that delivers an exact solution to (1 - 2) at t (more on this in subsection below). We can do this by equating the number of newly discovered cases in the NS population less the number of those newly vaccinated to the instantaneous decline in the susceptible population[3]:

$$dI_+(t) = \lim_{\Delta t \to 0} I(t + \Delta t) - I(t) = -dS(t) - dV(t) \; . \tag{3}$$

Eq. (3) applies to the CCL population as well.

Numerical solution of the SIR equations

Conventionally, (1 - 2) are solved numerically using the 4-th order explicit Runge-Kutta method [7]:

$$k_1 = -\left(\beta(t)S(t)I(t) + V(t)\right) \; , \tag{4}$$
$$l_1 = \left(\beta(t)S(t) - \gamma\right) I(t) \; , \tag{5}$$
$$k_2 = -\left[\beta(t)\left(S(t) + \frac{h}{2}k_1\right)\left(I(t) + \frac{h}{2}l_1\right) + V(t)\right] \; , \tag{6}$$
$$l_2 = \left[\beta(t)\left(S(t) + \frac{h}{2}k_1\right) - \gamma\right]\left[I(t) + \frac{h}{2}l_1\right] \; , \tag{7}$$
$$k_3 = -\left[\beta(t)\left(S(t) + \frac{h}{2}k_2\right)\left(I(t) + \frac{h}{2}l_2\right) + V(t)\right] \; , \tag{8}$$

[1] While this was certainly not the case initially, the accuracy of that number increase over time as testing became more prevalent and comprehensive; moreover, it is fair to assume that those inaccurate numbers reflected the qualitative dynamic of the pandemic.

[2] Initially, piecewise-constant; subsequently, polynomial or 7-day moving average

[3] Since susceptible population is monotonically decreasing, i.e., $dS(t) < 0$, $-dS(t) > 0$ represents the number of patients who have been infected or vaccinated at time t.

$$l_3 = \left[\beta(t)\left(S(t) + \frac{h}{2}k_2\right) - \gamma\right]\left[I(t) + \frac{h}{2}l_2\right] \ , \tag{9}$$

$$k_4 = -\left[\beta(t)(S(t) + hk_3)(I(t) + hl_3) + V(t)\right] \ , \tag{10}$$

$$l_4 = \left[\beta(t)\left(S(t) + hk_3\right) - \gamma\right]\left[I(t) + hl_3\right] \ , \tag{11}$$

$$S(t+h) = S(t) + \frac{h}{6}\left[k_1 + 2k_2 + 2k_3 + k_4\right] \ , \tag{12}$$

$$I(t+h) = I(t) + \frac{h}{6}\left[l_1 + 2l_2 + 2l_3 + l_4\right] \ . \tag{13}$$

The Runge-Kutta method (4 - 13) is explicit and therefore inherently unstable, however, it is conventionally applied for $h = 1$. The justification of this can be found, e.g., in [8].

Estimating the number of potential NS patients

Eq. (1 - 2) are written in terms of population percentages, i.e.,

$$S(t) = \frac{\mathcal{S}(t)}{N(t)} \ , \tag{14}$$

$$I(t) = \frac{\mathcal{I}(t)}{N(t)} \ , \tag{15}$$

$$V(t) = \frac{\mathcal{V}(t)}{N(t)} \ , \tag{16}$$

where

$\mathcal{S}(t)$ - NS population susceptible to the disease,

$\mathcal{I}(t)$ - NS population currently infected with the disease,

$\mathcal{V}(t)$ - NS population that has been vaccinated,

$N(t)$ - NS population at time t.

In order to estimate $N(t)$, we assumed that the current proportion of NS cases relative to the observed CCL cases is indicative of the fraction of the CCL population that potential NS patients represent. In other words,

$$\frac{\Delta\mathcal{I}_{+\mathcal{NS}}(t)}{\Delta I_{+CCL}(t)} = \frac{N(t)}{N_{CCL}} \ , \tag{17}$$

where

$\Delta\mathcal{I}_{+NS}(t)$ - newly discovered NS cases at time t,

$\Delta\mathcal{I}_{+CCL}(t)$ - newly discovered CCL cases at time t,

N_{CCL} - CCL population (deemed constant).

The left hand side of (17) is time-dependent. This seemingly contradicts the static assumption for N implied by the form of (1 - 2). One could, at least partially, refute this objection by pointing out that N is an *estimate at time t* of the true NS population. It is presumed to approach the exact (steady-state) value asymptotically. In fact, as can be inferred from Fig 1, empirical data suggests exponential decay of $\frac{N}{N_{CCL}}$ that can be approximated by

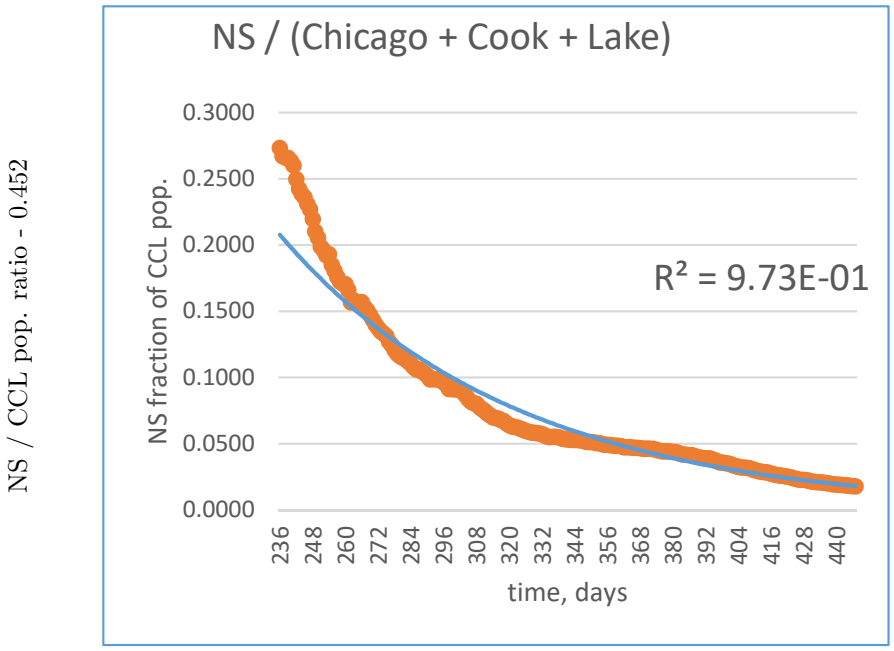

Fig 1. The ratio of NS and CCL populations. *x-axis*: elapsed time in days since March 10, 2020 (first identified NS case); *y-axis*: NS / CCL population ratio less 0.452 (asymptotic limit).

$$\frac{N}{N_{CCL}}(t) = \alpha + \beta e^{\mu t}\ , \tag{18}$$

where

$\alpha > 0, \beta > 0, \mu < 0$ - empirically determined constants[1]:
$\alpha = 0.452, \beta = 1.61, \mu = -0.012.$

U.S. Census Bureau [9] estimates the population of the CCL area to be 5,846,768 residents as of July 2019[2]. From (18), we can obtain the population estimate for NS to be approximately 392,000.

Projecting the number of hospitalizations, ICU and vent placements and deaths

In order to forecast the number of patients requiring general beds, ICU placement or intubation, we assume that, at any given time, a patient can be observed in any of the following states:

- on the floor but not in the ICU (and not intubated; lower acuity);
- in the ICU but not intubated (elevated acuity),

[1]The presented empirical fit was performed on the data between Oct. 31, 2020 and May 30, 2021.
[2]The latest data available at the time of writing.

– intubated (highest acuity).

The flowchart in Fig. 2 represents the progression of a hospitalized patient through his or her stay in the hospital. The following simplifying assumptions have been made:

– floor (lower acuity), ICU and intubated patients are accounted for separately, i.e., those are mutually exclusive groups;

– a patient is initially placed on the floor. If their condition is grave, transfer to ICU and / or intubation occurs (almost) instantly;

– upon deterioration, a patient proceeds from the floor to the ICU to intubation. No stages in this sequence are skipped, but a patient can spend almost no time in any state and be transferred to a higher acuity stage instantly[1];

– upon improvement, a patient proceeds from intubation to the ICU to the floor as applicable. No stages in this sequence are skipped but a patient can spend almost no time and be transferred to a lower acuity stage instantly;

– there is no formal restriction on how many times a patient can deteriorate or improve.

Under those assumptions, the state equations describing the population dynamics inside the hospital are

$$H_F(t) = \begin{cases} \dfrac{\mathcal{H}_{+F}(t;N_F)}{\mathcal{I}_{+NS}(t;N_F)} = \dfrac{\sum_{i=0}^{N_F-1}\Delta\mathcal{H}_{+F}(t_i)}{\sum_{i=0}^{N_F-1}\Delta\mathcal{I}_{+NS}(t_i)}, & T_0 <= t_0 < t_{N_F-1} <= T\ , \\ \dfrac{1}{N_F}\sum_{i=0}^{N_F-1} H_F(t_i), & t_{N_F-1} > T \end{cases}, \tag{19}$$

$$H_{ICU}(t) = \begin{cases} \dfrac{\mathcal{H}_{+ICU}(t;N_{ICU})}{\mathcal{H}_{+F}(t;N_{ICU})} = \dfrac{\sum_{i=0}^{N_{ICU}-1}\Delta\mathcal{H}_{+ICU}(t_i)}{\sum_{i=0}^{N_{ICU}-1}\Delta\mathcal{H}_{+F}(t_i)}, & T_0 <= t_0 < t_{N_{ICU}-1} <= T\ , \\ \dfrac{1}{N_{ICU}}\sum_{i=0}^{N_{ICU}-1} H_{ICU}(t_i), & t_{N_{ICU}-1} > T \end{cases}, \tag{20}$$

$$H_{vent}(t) = \begin{cases} \dfrac{\mathcal{H}_{+vent}(t;N_{vent})}{\mathcal{H}_{+ICU}(t;N_{vent})} = \dfrac{\sum_{i=0}^{N_{vent}-1}\Delta\mathcal{H}_{+vent}(t_i)}{\sum_{i=0}^{N_{vent}-1}\Delta\mathcal{H}_{+ICU}(t_i)}, & T_0 <= t_0 < t_{N_{vent}-1} <= T\ , \\ \dfrac{1}{N_{vent}}\sum_{i=0}^{N_{vent}-1} H_{vent}(t_i), & t_{N_{vent}-1} > T \end{cases}, \tag{21}$$

$$t_i = t_{i-1} + \Delta t\ .$$

where

N_F - length of lookback period for floor patients (at the time of this writing, 14 days),

[1] In other words, if a severely ill patient expires without being transferred to the ICU and / or being intubated, we consider that patient to have instantaneously transitioned through those two stages to mortality.

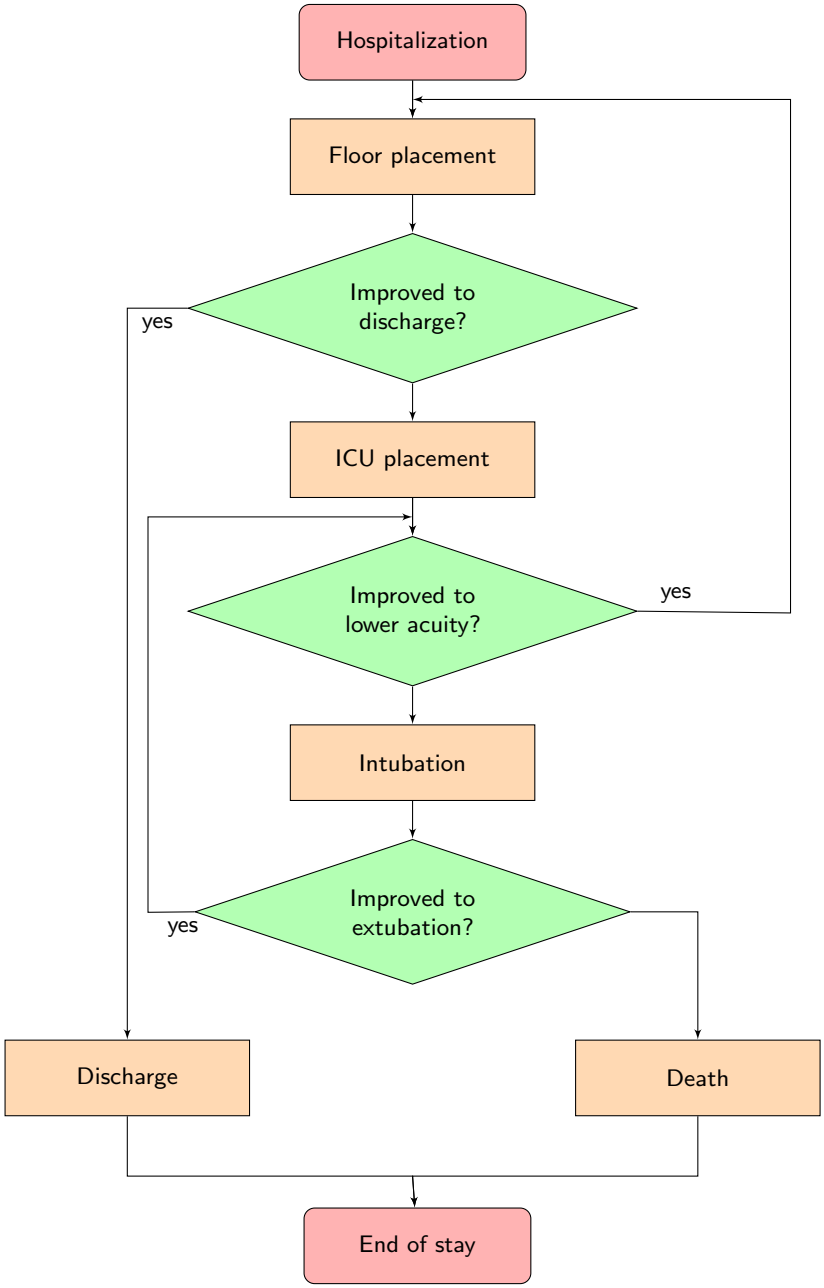

Fig 2. Progression of a hospitalized patient through their stay.

N_{ICU} - length of lookback period for ICU patients (14 days),

N_{vent} - length of lookback period for ventilated patients (14 days),

$H_F(t)$ - hospitalization rate at time t,

$\mathcal{H}_{+F}(t; N_F)$ - total number of new patients placed on the floor during the lookback period N_F,

$\mathcal{I}_{+NS}(t; N_F)$ - total number of new infections identified among NS patients during lookback period N_F,

$H_{ICU}(t)$ - ICU placement rate at time t,

$\mathcal{H}_{+ICU}(t; N_{ICU})$ - total number of new patients placed in the ICU during lookback period N_{ICU},

$\mathcal{H}_{+F}(t; N_{ICU})$ - total number of new patients placed on the floor during the lookback period N_{ICU},

$H_{vent}(t)$ - intubation rate at time t,

$\mathcal{H}_{+vent}(t; N_{vent})$ - total number of new patients placed on the ventilator during lookback period N_{vent},

$\mathcal{H}_{+ICU}(t; N_{vent})$ - total number of new patients placed on the floor during the lookback period N_{vent},

$\Delta\mathcal{H}_{+F}(t)$ - number of new patients placed on the floor at time t,

$\Delta\mathcal{H}_{+ICU}(t)$ - number of new patients placed in the ICU at time t,

$\Delta\mathcal{H}_{+vent}(t)$ - number of new intubations at time t,

T_0 - time of the start of the pandemic,

T - time of observation ("today").

Setting $t = t_{N_F} = t_{N_{ICU}} = t_{N_{vent}}$, i.e., setting the length of the lookback period N_B to be the same for all three groups of patients, $N_B \equiv N_F = N_{ICU} = N_{vent}$ reduces (19 - 21) to

$$H_F(t) = \begin{cases} \dfrac{\mathcal{H}_{+F}(t; N_B)}{\mathcal{I}_{+NS}(t; N_B)}, & T_0 <= t_0 < t_{N_B-1} <= T \\ \dfrac{1}{N_B} \displaystyle\sum_{i=0}^{N_B-1} H_F(t_i), & t_{N_F-1} > T \end{cases}, \tag{22}$$

$$H_{ICU}(t) = \begin{cases} \dfrac{\mathcal{H}_{+ICU}(t; N_B)}{\mathcal{H}_{+F}(t; N_B)}, & T_0 <= t_0 < t_{N_B-1} <= T \\ \dfrac{1}{N_B} \displaystyle\sum_{i=0}^{N_B-1} H_{ICU}(t_i), & t_{N_B-1} > T \end{cases}, \tag{23}$$

$$H_{vent}(t) = \begin{cases} \dfrac{\mathcal{H}_{+vent}(t; N_B)}{\mathcal{H}_{+ICU}(t; N_B)}, & T_0 <= t_0 < t_{N_B-1} <= T \\ \dfrac{1}{N_B} \displaystyle\sum_{i=0}^{N_B-1} H_{vent}(t_i), & t_{N_B-1} > T \end{cases}. \tag{24}$$

In other words, hospitalization, ICU and vents rates are computed exactly as rolling N-day averages up until the current time, and then extrapolated as averages over the same time period going forward[1].

The numbers of hospitalizations, ICU and vent placements are specific to the population served by a healthcare system and can be extrapolated to other entities only with caution. At the beginning of the pandemic, state-wide and regional data was either not available or unreliable thus necessitating an approximation using NS census and deaths. In doing so, the number of patients entering the hospital floor, ICU units and being intubated was assumed to be proportional to the observed number of cases.

In order to predict the counts (censuses) of the patient population currently hospitalized, placed in the ICU and intubated, it is necessary to model the flow of patients through each of those units. This can be done by backing out ("bootstrapping") recovery rates from the observed population dynamics as follows:

$$\mathcal{H}_F(T) = \mathcal{H}_F(T-\Delta T) + \Delta\mathcal{H}_{+F}(t) - \Delta\mathcal{H}_{-F}(t)\ , \tag{25}$$
$$\mathcal{H}_{ICU}(T) = \mathcal{H}_{ICU}(T-\Delta T) + \Delta\mathcal{H}_{+ICU}(t) - \Delta\mathcal{H}_{-ICU}(t)\ , \tag{26}$$
$$\mathcal{H}_{vent}(T) = \mathcal{H}_{vent}(T-\Delta T) + \Delta\mathcal{H}_{+vent}(t) - \Delta\mathcal{H}_{-vent}(t)\ , \tag{27}$$
$$\Delta\mathcal{H}_{+F}(t) = H_F(t)\Delta\mathcal{I}_{+NS}(t)\ , \tag{28}$$
$$\Delta\mathcal{H}_{+ICU}(t) = H_{ICU}(t)\Delta\mathcal{H}_{+F}(t)\ , \tag{29}$$
$$\Delta\mathcal{H}_{+vent}(t) = H_{vent}(t)\Delta\mathcal{H}_{+ICU}(t)\ , \tag{30}$$
$$\Delta\mathcal{H}_{-F}(t) = (\mu_F(t)-1)\mathcal{H}_{-F}(t-\Delta t) + \mathcal{H}_{-F}(t)\ , \tag{31}$$
$$\Delta\mathcal{H}_{-ICU}(t) = (\mu_{ICU}(t)-1)\mathcal{H}_{-ICU}(t-\Delta t) + \mathcal{H}_{-ICU}(t)\ , \tag{32}$$
$$\Delta\mathcal{H}_{-vent}(t) = (\mu_{vent}(t)-1)\mathcal{H}_{-vent}(t-\Delta t) + \mathcal{H}_{-vent}(t)\ , \tag{33}$$

where

$\mathcal{H}_F(T)$ - floor census at time t,

$\mathcal{H}_{ICU}(t)$ - ICU census at time t,

$\mathcal{H}_{vent}(t)$ - number of ventilated patients at time t.

$H_F(t)$ - hospitalization rate at time t,

$H_{ICU}(t)$ - ICU placement rate at time t,

$H_{vent}(t)$ - intubation rate at time t,

$\Delta\mathcal{H}_{-F}(t)$ - number of patients removed[2] from the floor at time t,

$\Delta\mathcal{H}_{-ICU}(t)$ - number of patients removed[3] from the ICU at time t,

$\Delta\mathcal{H}_{-vent}(t)$ - number of extubations[4] at time t,

N_F - length of lookback period for floor patients (at the time of this writing, 7 days),

N_{ICU} - length of lookback period for ICU patients (7 days),

N_{vent} - length of lookback period for intubated patients (14 days),

[1] It does not appear possible to define those rates smoothly since the calculation of the rate itself depends on the predicted number of affected patients which, in turn, depends on the rate creating a "circular reference".

[2] Due to discharge, placement in the ICU or death.

[3] Due to return to the general floor population, intubation or death.

[4] Due to extubation or death.

$\mu_F(t)$ - observed floor removal rate at time t,

$\mu_{ICU}(t)$ - observed ICU placement rate at time t,

$\mu_{vent}(t)$ - observed extubation rate at time t.

Eq. (31 - 33) can be used to determine the values of μ_F, μ_{ICU} and μ_{vent} for $t \leq T$. For $t > T$, moving average extrapolations are used (cf.(22 - 24)):

$$\mu_F(t) = \frac{1}{N_F} \sum_{i=0}^{N_F-1} \mu_F(t_i) \ , \tag{34}$$

$$\mu_{ICU}(t) = \frac{1}{N_{ICU}} \sum_{i=0}^{N_{ICU}-1} \mu_{ICU}(t_i) \ , \tag{35}$$

$$\mu_{vent}(t) = \frac{1}{N_{vent}} \sum_{i=0}^{N_{vent}-1} \mu_{vent}(t_i) \ , \tag{36}$$

$$t \equiv t_{N_F} \equiv t_{N_{ICU}} \equiv t_{N_{vent}} \ , t_i = t_{i-1} + \Delta t \ .$$

Following the patient flow assumptions reflected in Fig. 1, mortality rate is computed as

$$M(t) = \frac{\sum_{i=0}^{N} \mathcal{M}(t_i)}{\sum_{i=0}^{N} \mathcal{H}_{ICU}(t_i)} \ , \tag{37}$$

where

$M(t)$ - mortality rate at time t,

$\mathcal{M}(t)$ - cumulative number of deaths at time t,

$t \equiv t_N$ - current time .

Projecting vaccination rates

Vaccination rates in the CCL area at the time of this writing followed a quartic trajectory with remarkable accuracy, as shown in Fig. 3.

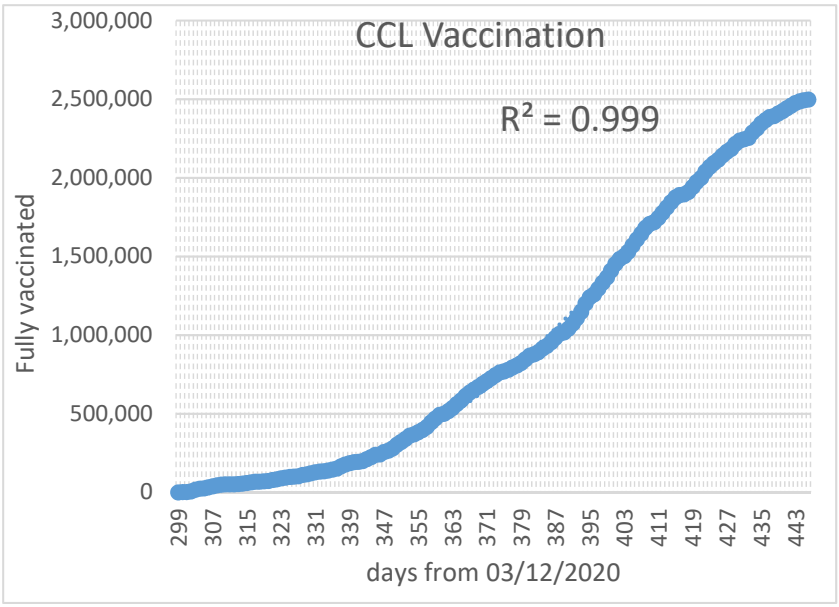

Fig 3. CCL vaccination rates, Jan. 3. - May 30, 2021.

Empirically, the shape of the quartic parabola is determined using the usual least squares best fit to be[1]

$$\mathcal{V}^{(4)}_{CCL}(t) = -5.667435 \times 10^{-3}\, t^4 + 7.590466\, t^3 - 3.619223 \times 10^3\, t^2 + 7.302425 \times 10^5\, t - 5.232056 \times 10^7\ . \tag{38}$$

Imposing the upper limit of 100% of the population and requiring that the number of vaccinated individuals be monotonically nondecreasing, we obtain[2]

$$\mathcal{V}_{CCL}(t) = \min\left[N_{CCL}, \max(\mathcal{V}^{(4)}_{CCL}(t), \mathcal{V}_{CCL}(t-\Delta t))\right]\ . \tag{39}$$

The number of fully vaccinated NS patients is then obtained from (18) as

$$\mathcal{V}_{NS}(t) = \frac{N}{N_{CCL}}\,(t)\,\mathcal{V}_{CCL}(t)\ . \tag{40}$$

Results and discussion

Worked example

In the example below, we assume that CCL population is 5,846,768, relevant NS patient population estimated by (18) is 392,000 and infection transmission period $1/\gamma = 15$. We set the pandemic start date to March 10, 2020.

[1] The number of significant digits here is extended for consistency.

[2] Based on the official CCL vaccination data from Jan. 3, 2021 to May 30, 2021.

The date for this example was arbitrarily chosen from past history with the requirements that the number of new cases, patient admissions and censuses on the floor, in the ICU and attached to a ventilator be reasonable large to avoid instability and that the trajectory of the pandemic be fairly well established.

NS case and admission data as of Feb. 26, 2021 is presented in Table 1.

The last row of the table is incomplete because, while reliable case data is generally available up to and including the next-but-last day, case and hospitalization data is relatively reliable for the preceding day.

Calculations for the Runge-Kutta implementation of the model for CCL as of Feb. 26, 2021 are presented in Table 2, and for NS they are displayed in 3.

With the line corresponding to the date of 2/24/2021 as an example, the algorithm proceeds as follows:

1. Using Excel Solver[1] (or any other optimization routine), find the value of β on the preceding day that minimizes the square of the residual between the predicted and observed number of cases at time t:

$$\beta(t_{i-1}) = argmin(\hat{\mathcal{I}}(t_0, t_i) - \mathcal{I}(t_0, t_i))^2 \,, \tag{41}$$

$$\begin{aligned}\hat{\mathcal{I}}(t_0, t_i) = \hat{\mathcal{I}}(t_0, t_{i-1}) + [(\mathcal{S}(t_i) - \mathcal{S}(t_{i-1}) \\ - (\mathcal{V}(t_{i-1}) - \mathcal{V}(t_{i-2}))]\, N(t_i) \,, i = \overline{2, L} \,, t_L \equiv t \,,\end{aligned} \tag{42}$$

where

$\hat{\mathcal{I}}(t_0, t_i)$ - *predicted* cumulative number of identified positive cases from the beginning of the pandemic t_0 to time t_i,

$\mathcal{I}(t_0, t_i)$ - *actual* cumulative number of identified positive case from the beginning of the pandemic t_0 to time t_i,

$N(t)$ - NS population at time t_i (i.e., the asymptotic limit of (18) .

t_i - current time at the i-th time step.

The value of β at which this minimum is achieved corresponds to the preceding time step, 2/23/2021, and is equal to 0.043[2].

2. Compute the transmission rate

$$R_0(t_i) = \frac{\beta}{\gamma} \,, i = \overline{2, L} \,, t_L \equiv t \,, \tag{43}$$

for future reference ($\frac{1}{\gamma} = 15$ days, $R_0 = 0.043 \times 15 = 0.65$).

3. Compute the NS susceptible rate (cf. 12)

$$S(t_i) = S(t_{i-1}) + k(t_{i-1})dt \,, \tag{44}$$

$$k(t_{i-1}) = \frac{h}{6}\left[k_1(t_{i-1}) + 2k_2(t_{i-1}) + 2k_3(t_{i-1}) + k_4(t_{i-1})\right] \,, \tag{45}$$

$$h = t_i - t_{i-1} \,, i = \overline{2, L} \,, t_L \equiv t \,.$$

The above yields $S(t_i) = 0.8604 - 6.35 \times 10^{-4} \times 1 = 0.8598$.

[1] unconstrained GRG nonlinear optimization using centered difference approximation and automatic scaling with constraint precision = convergence tolerance = 10^{-3}.

[2] Rounded to two significant digits.

Date	Chicago+Cook+Lake CCL Cases	CCL Vac	NorthShore NS act cases	NS Vac	NS act. Inp.	NS act. Inp. Cen-sus	NS act. ICU	Ns act. add'l ICU	NS act ICU only	GAU	NS act. ICU cen-sus	Ns act. ICU rate	NS act. Vent	Ns act. add'l vent	NS act. vent cen-sus	Ns act. vent rate	NS act. Mort.	NS Mort. Rate	act.
2/1/2021	510592	106260	35701	7430	2,899	61	546	0	8	0	8	0.12	270	0	5	0.38	496	0.908	
2/2/2021	511409	110902	35748	7752	2,910	58	548	2	9	0	9	0.14	272	2	6	0.44	498	0.909	
2/3/2021	512613	117264	35808	8191	2,920	54	549	1	9	0	9	0.13	272	0	5	0.41	500	0.911	
2/4/2021	513929	122009	35861	8514	2,926	51	553	4	11	0	11	0.21	273	1	5	0.3	502	0.908	
2/5/2021	515469	126389	35901	8803	2,931	49	554	1	10	0	10	0.18	276	3	7	0.4	502	0.906	
2/6/2021	516772	127857	35942	8893	2,940	51	555	1	10	0	10	0.18	277	1	7	0.47	503	0.906	
2/7/2021	517677	132925	35967	9235	2,943	49	555	0	9	0	9	0.16	277	0	6	0.44	504	0.908	
2/8/2021	518344	138618	36022	9633	2,953	52	556	1	9	0	9	0.19	277	0	5	0.47	505	0.908	
2/9/2021	519080	146292	36074	10167	2,960	49	557	1	9	0	9	0.18	277	0	4	0.41	506	0.908	
2/10/2021	520153	159414	36124	11071	2,967	45	558	1	8	0	8	0.19	278	1	3	0.47	508	0.910	
2/11/2021	521218	171525	36155	11898	2,976	45	559	1	7	0	7	0.12	278	0	3	0.44	509	0.911	
2/12/2021	522383	179935	36190	12466	2,982	43	560	1	7	0	7	0.12	278	0	2	0.5	510	0.911	
2/13/2021	523254	184662	36228	12785	2,987	43	560	0	7	0	7	0.11	279	1	3	0.6	511	0.913	
2/14/2021	523920	187490	36256	12975	2,994	45	560	0	6	0	6	0.1	279	0	1	0.64	513	0.916	
2/15/2021	524508	192601	36288	13325	2,999	45	562	2	8	0	8	0.13	280	1	2	0.63	513	0.913	
2/16/2021	525044	203676	36319	14089	3,003	43	562	0	8	0	8	0.12	280	0	2	0.57	514	0.915	
2/17/2021	525722	217944	36358	15073	3,008	37	562	0	8	0	8	0.1	280	0	2	0.62	515	0.916	
2/18/2021	526379	231601	36391	16012	3,016	37	564	2	9	0	9	0.13	280	0	2	0.64	516	0.915	
2/19/2021	527198	234098	36425	16174	3,018	31	565	1	8	0	8	0.14	281	1	3	0.45	516	0.913	
2/20/2021	527997	248822	36437	17171	3,020	27	565	0	8	0	8	0.15	281	0	3	0.4	518	0.917	
2/21/2021	528646	257625	36456	17766	3,025	30	565	0	5	0	5	0.16	281	0	2	0.4	519	0.919	
2/22/2021	529161	271716	36494	18739	3,032	34	567	2	7	0	7	0.15	284	3	5	0.64	519	0.915	
2/23/2021	529797	293847	36520	20255	3,035	34	567	0	7	0	7	0.16	284	0	5	0.7	519	0.915	
2/24/2021	530681					30		0	6					0	4		519		

Table 1. NS COVID-19 case and admission data, Feb. 1 - 24, 2021.

Date	Beta	R0	CCL Sus-cept rate	CCL Vac rate	Inf rate	k1	l1	k2	l2	k3	l3	k4	l4	k	l
2/1/2021	0.031	0.472	0.8958	0.018	0.0051	-1.05E-03	-1.02E-04	-1.05E-03	-1.02E-04	-1.05E-03	-1.02E-04	-1.04E-03	-1.01E-04	-1.05E-03	-1.02E-04
2/2/2021	0.048	0.718	0.8947	0.019	0.0050	-1.01E-03	-1.18E-04	-1.00E-03	-1.17E-04	-1.00E-03	-1.17E-04	-1.00E-03	-1.17E-04	-1.00E-03	-1.17E-04
2/3/2021	0.054	0.803	0.8937	0.020	0.0048	-1.32E-03	-9.11E-05	-1.32E-03	-9.05E-05	-1.32E-03	-9.05E-05	-1.32E-03	-9.05E-05	-1.32E-03	-9.06E-05
2/4/2021	0.064	0.955	0.8924	0.021	0.0048	-1.08E-03	-4.69E-05	-1.08E-03	-4.69E-05	-1.08E-03	-4.69E-05	-1.08E-03	-4.69E-05	-1.08E-03	-4.69E-05
2/5/2021	0.055	0.820	0.8913	0.022	0.0047	-9.78E-04	-8.44E-05	-9.76E-04	-8.38E-05	-9.76E-04	-8.38E-05	-9.76E-04	-8.38E-05	-9.77E-04	-8.39E-05
2/6/2021	0.039	0.584	0.8903	0.022	0.0046	-4.11E-04	-1.48E-04	-4.09E-04	-1.45E-04	-4.09E-04	-1.45E-04	-4.09E-04	-1.45E-04	-4.09E-04	-1.46E-04
2/7/2021	0.030	0.447	0.8899	0.023	0.0045	-9.85E-04	-1.80E-04	-9.83E-04	-1.76E-04	-9.83E-04	-1.76E-04	-9.83E-04	-1.76E-04	-9.83E-04	-1.77E-04
2/8/2021	0.034	0.513	0.8889	0.024	0.0043	-1.10E-03	-1.56E-04	-1.10E-03	-1.53E-04	-1.10E-03	-1.53E-04	-1.10E-03	-1.53E-04	-1.10E-03	-1.54E-04
2/9/2021	0.051	0.771	0.8878	0.025	0.0041	-1.50E-03	-8.72E-05	-1.50E-03	-8.65E-05	-1.50E-03	-8.65E-05	-1.50E-03	-8.65E-05	-1.50E-03	-8.66E-05
2/10/2021	0.052	0.783	0.8863	0.027	0.0041	-2.43E-03	-8.28E-05	-2.43E-03	-8.23E-05	-2.43E-03	-8.23E-05	-2.43E-03	-8.23E-05	-2.43E-03	-8.24E-05
2/11/2021	0.058	0.874	0.8839	0.029	0.0040	-2.28E-03	-6.03E-05	-2.27E-03	-6.01E-05	-2.27E-03	-6.01E-05	-2.27E-03	-6.01E-05	-2.27E-03	-6.01E-05
2/12/2021	0.045	0.669	0.8816	0.031	0.0039	-1.59E-03	-1.07E-04	-1.59E-03	-1.06E-04	-1.59E-03	-1.06E-04	-1.59E-03	-1.06E-04	-1.59E-03	-1.06E-04
2/13/2021	0.035	0.529	0.8800	0.032	0.0038	-9.27E-04	-1.36E-04	-9.24E-04	-1.33E-04	-9.24E-04	-1.33E-04	-9.24E-04	-1.33E-04	-9.25E-04	-1.34E-04
2/14/2021	0.032	0.485	0.8791	0.032	0.0037	-5.88E-04	-1.41E-04	-5.86E-04	-1.38E-04	-5.86E-04	-1.38E-04	-5.86E-04	-1.38E-04	-5.86E-04	-1.38E-04
2/15/2021	0.031	0.460	0.8785	0.033	0.0035	-9.69E-04	-1.41E-04	-9.67E-04	-1.38E-04	-9.68E-04	-1.38E-04	-9.68E-04	-1.38E-04	-9.68E-04	-1.38E-04
2/16/2021	0.040	0.604	0.8776	0.035	0.0034	-2.01E-03	-1.07E-04	-2.01E-03	-1.05E-04	-2.01E-03	-1.05E-04	-2.01E-03	-1.05E-04	-2.01E-03	-1.05E-04
2/17/2021	0.040	0.605	0.8755	0.037	0.0033	-2.56E-03	-1.03E-04	-2.55E-03	-1.02E-04	-2.55E-03	-1.02E-04	-2.55E-03	-1.02E-04	-2.56E-03	-1.02E-04
2/18/2021	0.052	0.777	0.8730	0.040	0.0032	-2.48E-03	-6.84E-05	-2.48E-03	-6.79E-05	-2.48E-03	-6.79E-05	-2.48E-03	-6.79E-05	-2.48E-03	-6.80E-05
2/19/2021	0.052	0.776	0.8705	0.040	0.0031	-5.68E-04	-6.76E-05	-5.66E-04	-6.69E-05	-5.66E-04	-6.69E-05	-5.66E-04	-6.69E-05	-5.66E-04	-6.70E-05
2/20/2021	0.043	0.648	0.8699	0.043	0.0031	-2.63E-03	-8.89E-05	-2.63E-03	-8.78E-05	-2.63E-03	-8.78E-05	-2.63E-03	-8.78E-05	-2.63E-03	-8.80E-05
2/21/2021	0.035	0.532	0.8673	0.044	0.0030	-1.60E-03	-1.07E-04	-1.60E-03	-1.05E-04	-1.60E-03	-1.05E-04	-1.60E-03	-1.05E-04	-1.60E-03	-1.05E-04
2/22/2021	0.045	0.680	0.8657	0.046	0.0029	-2.52E-03	-7.85E-05	-2.52E-03	-7.76E-05	-2.52E-03	-7.76E-05	-2.52E-03	-7.76E-05	-2.52E-03	-7.77E-05
2/23/2021	0.064	0.967	0.8629	0.047	0.0027	-7.26e-04	-3.02E-05	-7.25e-04	-3.01E-05	-7.25e-04	-3.01E-05	-7.24e-04	-3.00E-05	-7.25E-04	-3.01E-05
2/24/2021	0.048	0.721	0.8622	0.054	0.0027	-7.50e-03	-6.84E-05	-7.50e-03	-6.80E-05	-7.50e-03	-6.80E-05	-7.50e-03	-6.76E-05	-7.50e-03	-6.80E-05

Table 2. Runge-Kutta implementation for the CCL COVID-19 model, Feb. 1 - 24, 2021.

Date	Day	NS beta	NS R0	NS Sus-cept rate	Vac Rate	Not sus-cept #	Inf rate	Inf #	Inf cu-mul	NS pred hosp rate	Cu-mul hosp #	Ho-sp Δ	NS inp disch rate	IP cen-sus	NS pred ICU rate	Cu-mul ICU #	ICU Δ	NS ICU disch rate	ICU cen-sus	NS pred vent rate	Cu-mul Vent #	Vent ?
2/1/21	321	0.046	0.70	0.8921	0.018	42,315	2.94E-03	1,151	35,683	0.135	2905	11	0.167	61	0.138	546	0	0.11	8	0.38	270	0
2/2/21	322	0.060	0.91	0.8907	0.019	42,854	2.86E-03	1,122	35,730	0.138	2916	11	0.230	58	0.140	548	2	0.125	9	0.44	272	2
2/3/21	323	0.054	0.81	0.8897	0.020	43,225	2.83E-03	1,108	35,790	0.143	2926	10	0.241	54	0.145	549	1	0.111	9	0.41	272	0
2/4/21	324	0.042	0.63	0.8885	0.021	43,705	2.77E-03	1,088	35,843	0.146	2932	6	0.167	51	0.174	553	4	0.222	11	0.30	273	1
2/5/21	325	0.044	0.67	0.8876	0.022	44,063	2.69E-03	1,056	35,883	0.151	2937	5	0.137	49	0.179	554	1	0.182	10	0.40	276	3
2/6/21	326	0.028	0.42	0.8867	0.022	44,398	2.62E-03	1,028	35,924	0.156	2946	9	0.143	51	0.167	555	1	0.100	10	0.47	277	1
2/7/21	327	0.063	0.95	0.8864	0.023	44,521	2.51E-03	986	35,949	0.153	2949	3	0.098	49	0.167	555	0	0.100	9	0.44	277	0
2/8/21	328	0.062	0.93	0.8854	0.024	44,916	2.49E-03	975	36,004	0.160	2959	10	0.143	52	0.153	556	1	0.111	9	0.47	277	0
2/9/21	329	0.059	0.89	0.8843	0.025	45,351	2.46E-03	964	36,057	0.159	2966	7	0.192	49	0.156	557	1	0.111	9	0.41	277	0
2/10/21	330	0.038	0.56	0.8829	0.027	45,915	2.42E-03	950	36,107	0.159	2973	7	0.224	45	0.159	558	1	0.222	8	0.47	278	1
2/11/21	331	0.044	0.66	0.8805	0.029	46,826	2.34E-03	919	36,138	0.164	2982	9	0.200	45	0.168	559	1	0.250	7	0.44	278	0
2/12/21	332	0.049	0.74	0.8784	0.031	47,673	2.28E-03	893	36,173	0.175	2989	7	0.178	44	0.150	560	1	0.143	7	0.50	278	0
2/13/21	333	0.037	0.56	0.8768	0.032	48,275	2.23E-03	872	36,211	0.170	2994	5	0.114	44	0.144	560	0	0.000	7	0.60	279	1
2/14/21	334	0.044	0.66	0.8760	0.032	48,620	2.15E-03	843	36,239	0.177	3001	7	0.136	45	0.131	560	0	0.143	6	0.64	279	0
2/15/21	335	0.042	0.64	0.8754	0.033	48,841	2.09E-03	820	36,271	0.172	3006	5	0.111	45	0.158	562	2	0.000	8	0.63	280	1
2/16/21	336	0.057	0.85	0.8745	0.035	49,214	2.03E-03	796	36,301	0.165	3010	4	0.133	43	0.149	562	0	0.000	8	0.57	280	0
2/17/21	337	0.049	0.74	0.8725	0.037	49,996	2.00E-03	782	36,340	0.162	3015	5	0.256	37	0.146	562	0	0.000	8	0.62	280	0
2/18/21	338	0.050	0.75	0.8699	0.040	50,985	1.95E-03	764	36,373	0.172	3023	8	0.216	37	0.121	564	2	0.125	9	0.64	280	0
2/19/21	339	0.019	0.29	0.8675	0.040	51,934	1.90E-03	746	36,406	0.168	3025	2	0.216	31	0.125	565	1	0.222	8	0.45	281	1
2/20/21	340	0.032	0.47	0.8671	0.043	52,113	1.81E-03	710	36,418	0.164	3027	2	0.194	27	0.123	565	0	0.000	8	0.40	281	0
2/21/21	341	0.065	0.97	0.8645	0.044	53,119	1.74E-03	682	36,437	0.170	3032	5	0.074	30	0.12	565	0	0.375	5	0.40	281	0
2/22/21	342	0.045	0.68	0.8629	0.046	53,748	1.72E-03	675	36,475	0.172	3040	8	0.100	35	0.136	567	2	0.000	7	0.64	284	3
2/23/21	343	0.043	0.65	0.8604	0.047	54,718	1.68E-03	657	36,501	0.173	3043	3	0.086	35	0.13	567	0	0.000	7	0.70	284	0
2/24/21	344	0.061	0.91	0.8598	0.054	54,967	1.63E-03	638	36,525	0.169	3044	1	0.170	30	0.140	568	1	0.106	7	0.55	284	0

Table 3. Runge-Kutta implementation for the NS COVID-19 model, Feb. 1 - 24, 2021.

Date	NS vent disch rate	Vent cen- sus	NS pr- ed mo- rt rate	NS pr- ed mo- rt	NS new inf	k1	l1	k2	l2	k3	l3	k4	l4	k	l
2/1/21	0.00	5	0.910	497	50	-1.38E-03	-7.42E-05	-1.38E-03	-7.34E-05	-1.38E-03	-7.34E-05	-1.38E-03	-7.25E-05	-1.38E-03	-7.34E-05
2/2/21	0.20	6	0.911	499	47	-9.48E-04	-3.67E-05	-9.47E-04	-3.65E-05	-9.47E-04	-3.65E-05	-9.46E-04	-3.64E-05	-9.47E-04	-3.65E-05
2/3/21	0.17	5	0.913	501	60	-1.22E-03	-5.19E-05	-1.22E-03	-5.15E-05	-1.22E-03	-5.15E-05	-1.22E-03	-5.11E-05	-1.22E-03	-5.15E-05
2/4/21	0.20	5	0.910	503	53	-9.15E-04	-8.14E-05	-9.14E-04	-8.02E-05	-9.14E-04	-8.02E-05	-9.12E-04	-7.91E-05	-9.14E-04	-8.02E-05
2/5/21	0.20	7	0.908	503	40	-8.55E-04	-7.35E-05	-8.54E-04	-7.26E-05	-8.54E-04	-7.26E-05	-8.52E-04	-7.17E-05	-8.54E-04	-7.26E-05
2/6/21	0.14	7	0.908	504	41	-3.16E-04	-1.10E-04	-3.15E-04	-1.07E-04	-3.15E-04	-1.07E-04	-3.14E-04	-1.05E-04	-3.15E-04	-1.07E-04
2/7/21	0.14	6	0.910	505	25	-1.01E-03	-2.65E-05	-1.01E-03	-2.64E-05	-1.01E-03	-2.64E-05	-1.01E-03	-2.64E-05	-1.01E-03	-2.64E-05
2/8/21	0.17	5	0.910	506	55	-1.11E-03	-2.98E-05	-1.11E-03	-2.97E-05	-1.11E-03	-2.97E-05	-1.11E-03	-2.96E-05	-1.11E-03	-2.97E-05
2/9/21	0.20	4	0.910	507	53	-1.44E-03	-3.53E-05	-1.44E-03	-3.52E-05	-1.44E-03	-3.52E-05	-1.44E-03	-3.50E-05	-1.44E-03	-3.52E-05
2/10/21	0.50	3	0.912	509	50	-2.32E-03	-8.10E-05	-2.32E-03	-7.98E-05	-2.32E-03	-7.98E-05	-2.32E-03	-7.86E-05	-2.32E-03	-7.98E-05
2/11/21	0.00	3	0.912	510	31	-2.16E-03	-6.56E-05	-2.16E-03	-6.48E-05	-2.16E-03	-6.48E-05	-2.16E-03	-6.40E-05	-2.16E-03	-6.48E-05
2/12/21	0.33	2	0.913	511	35	-1.54E-03	-5.37E-05	-1.54E-03	-5.32E-05	-1.54E-03	-5.32E-05	-1.53E-03	-5.26E-05	-1.54E-03	-5.32E-05
2/13/21	0.00	3	0.914	512	38	-8.81E-04	-7.57E-05	-8.80E-04	-7.44E-05	-8.80E-04	-7.44E-05	-8.79E-04	-7.32E-05	-8.80E-04	-7.44E-05
2/14/21	0.67	1	0.918	514	28	-5.67E-04	-6.06E-05	-5.65E-04	-5.97E-05	-5.65E-04	-5.98E-05	-5.64E-04	-5.89E-05	-5.65E-04	-5.98E-05
2/15/21	0.00	2	0.915	514	32	-9.52E-04	-6.17E-05	-9.51E-04	-6.08E-05	-9.51E-04	-6.08E-05	-9.50E-04	-6.00E-05	-9.51E-04	-6.08E-05
2/16/21	0.00	2	0.916	515	30	-1.99E-03	-3.49E-05	-1.99E-03	-3.47E-05	-1.99E-03	-3.47E-05	-1.99E-03	-3.45E-05	-1.99E-03	-3.47E-05
2/17/21	0.00	2	0.918	516	39	-2.53E-03	-4.77E-05	-2.52E-03	-4.73E-05	-2.52E-03	-4.73E-05	-2.52E-03	-4.68E-05	-2.52E-03	-4.73E-05
2/18/21	0.00	2	0.917	517	33	-2.42E-03	-4.46E-05	-2.42E-03	-4.42E-05	-2.42E-03	-4.42E-05	-2.42E-03	-4.38E-05	-2.42E-03	-4.42E-05
2/19/21	0.00	3	0.915	517	34	-4.58E-04	-9.55E-05	-4.58E-04	-9.32E-05	-4.58E-04	-9.32E-05	-4.57E-04	-9.09E-05	-4.58E-04	-9.32E-05
2/20/21	0.00	3	0.919	519	12	-2.57E-03	-7.12E-05	-2.57E-03	-6.99E-05	-2.57E-03	-6.99E-05	-2.57E-03	-6.86E-05	-2.57E-03	-6.99E-05
2/21/21	0.33	2	0.920	520	19	-1.60E-03	-1.85E-05	-1.60E-03	-1.85E-05	-1.60E-03	-1.85E-05	-1.60E-03	-1.85E-05	-1.60E-03	-1.85E-05
2/22/21	0.00	5	0.917	520	38	-2.48E-03	-4.75E-05	-2.48E-03	-4.69E-05	-2.48E-03	-4.69E-05	-2.48E-03	-4.64E-05	-2.48E-03	-4.69E-05
2/23/21	0.00	5	0.917	520	26	-6.35E-04	-4.95E-05	-6.35E-04	-4.88E-05	-6.35E-04	-4.88E-05	-6.34E-04	-4.81E-05	-6.35E-04	-4.88E-05
2/24/21	0.13	4	0.917	520	24	-7.48E-03	-2.35E-05	-7.47E-03	-2.37E-05	-7.47E-03	-2.37E-05	-7.47E-03	-2.39E-05	-7.47E-03	-2.37E-05

Table 3. (cont.) Runge-Kutta implementation for the NS COVID-19 model, Feb. 1 - 24, 2021.

4. Compute the NS vaccination rate from (39 - 40) and Table 3 [1]

$$\begin{aligned}\mathcal{V}_{\mathcal{CCL}}(t_i) = \min\{5,846,768; &- 5.667435 \times 10^{-3} \times 351^4 + 7.590466 \times 351^3 \\ &- 3.619223 \times 10^3 \times 351^2 + 7.302425 \times 10^5 \times 351 \\ &- 5.232056 \times 10^7\} = 318,279 \ , \\ V_{CCL}(t_i) = V_{NS}(t_i) &= \frac{318,279}{5,846,768} = 0.054437 \ , \\ \mathcal{V}_{NS}(t) &= 0.054437 \times 392,000 = 21,339 \ .\end{aligned}$$

5. Compute the number of patients who are no longer susceptible to the disease

$$\rho_{NS}(t_i) = (1 - S(t_i))N(t_i) = (1 - 0.8598) \times 392,000 = 54,967 \ ,$$

6. Compute the infection rate

$$I(t_i) = I(t_{i-1}) + l(t_{i-1})dt \ , \tag{46}$$

$$l(t_{i-1}) = \frac{h}{6}\left[l_1(t_{i-1}) + 2l_2(t_{i-1}) + 2l_3(t_{i-1}) + l_4(t_{i-1})\right] \ , \tag{47}$$

$$h = t_i - t_{i-1} \ , i = \overline{2, L} \ , t_L \equiv t \ .$$

The above yields $I(t_i) = 1.63 \times 10^{-3} - 4.88 \times 10^{-5} = 1.63 \times 10^{-3}$. 214

7. Compute the predicted cumulative number of positive cases from (42) to arrive at

$$\begin{aligned}\mathcal{I}(t_i) = 36,501 &+ \left[(0.86041 - 0.85978) - (0.0493 - 0.0470) \times 10^{-3}\right] \\ &\times 392,000 = 36,525 \ .\end{aligned}$$

The predicted number of new infections is[2] $36,525 - 36,501 = 24$. 215

8. Compute the predicted hospitalization rate from (22)

$$H_F(t_i) = 0.1687 \ .$$

9. Compute cumulative hospitalizations

$$\begin{aligned}\mathcal{H}_F(t_0; t_i) = \max(&\mathcal{H}_F(t_0; t_i), \mathcal{H}_F(t_0; t_{i-N_F}) + H_F(t_i)(\Delta\mathcal{I}(t_0; t_i) \\ &- \Delta\mathcal{I}(t_0; t_i - N_F))) = \max(3,043, 2,973 + 0.1687 \\ &\times (36,525 - 36,107)) = 3,044 \ .\end{aligned}$$

and $\Delta\mathcal{H}_{+F}(t_i) = 3,044 - 3,043 = 1$ new patient. 216

10. Compute the predicted floor removal rate from (34) : $\mu_F(t_i) = 0.170$. 217

11. Compute the predicted floor census from (25)

$$\mathcal{H}_F(t_i) = 4 + 35 \times (1 - 0.170) = 33 \ .$$

[1] Significant digits added for consistency

[2] In reality, this calculation is performed in reverse order.

12. Repeat steps 8 - 11 for ICU and vented patients to obtain from (26 - 29)

$$
\begin{aligned}
H_{ICU}(t_i) &= 0.140; , \\
\mathcal{H}_{ICU}(t_0;t_i) &= \max(\mathcal{H}_{ICU}(t_0;t_i), \mathcal{H}_{ICU}(t_0;t_{i-N_F}) \\
&\quad + H_{ICU}(t_i)(\mathcal{H}_{\mathcal{F}}(t_0;t_i) - \mathcal{H}_{\mathcal{F}}(t_0;t_i - N_F)) \\
&= \max(567, 558 + 0.140 \times (3,044 - 2,973)) = 568 , \\
\Delta\mathcal{H}_{+ICU}(t_i) &= 568 - 567 = 1 , \\
\mu_{ICU}(t_i) &= 0.106 , \\
\mathcal{H}_{ICU} &= 1 + 7 \times (1 - 0.106) = 7 , \\
\mathcal{H}_{vent}(t_0;t_i) &= \max(\mathcal{H}_{vent}(t_0;t_i), \mathcal{H}_{vent}(t_0;t_{i-N_F}) \\
&\quad + H_{vent}(t_i)(\mathcal{H}_{ICU}(t_0;t_i) - \mathcal{H}_{ICU}(t_0;t_i - N_F)) \\
&= \max(284, 278 + 0.55 \times (567 - 558)) = 284 , \\
\Delta\mathcal{H}_{+vent}(t_i) &= 284 - 284 = 0 , \\
\mu_{vent}(t_i) &= 0.130 , \\
\mathcal{H}_{vent} &= 0 + 5 \times (1 - 0.13) = 4 .
\end{aligned}
$$

13. Compute expected mortality rate and mortality from (37)

$$M(t_i) = \frac{\mathcal{M}(t_i)}{\mathcal{H}_{ICU}(t_0;t_i)} = \frac{520}{567} = 0.917 .$$

Model accuracy

An analysis of the accuracy of predictions was performed for the period starting on Mar. 10, 2020 and ending on May 24, 2021. Predictions were initially generated daily, then weekly, then twice a week, on Mondays and Thursdays with a few exceptions around statutory holiday. Forecasts produced between the periods of calculation were classified as "one-day-ahead" (even though they may have been issued 1 to 6 days in advance); one- and two-week-ahead predictions were also considered. Two sets of predictions were issued on each occasion: one based on the NS data, the other extrapolated from the CCL data adjusting for the then-current share that NS population represented in the CCL pool according to (17 - 18). The synthesis of two disparate sources required a different metric than, e.g., weighted interval score, employed for this purpose in [23], [22]. For practical purposes, we adopted a simplified approach described below[1].The minima and maxima of projections thus generated were considered the lower and upper forecast boundaries. If subsequently realized values fell within those boundaries, the corresponding error was set to zero, otherwise it was taken to be the absolute relative error of the most accurate boundary (upper or lower). The results are presented in Table 4. Evidently, the best predictions in terms for the number of positive cases, floor, ICU and vent censuses are achieved one day in advance, and the accuracy deteriorates with the increase in the time horizon. This was to be expected. The accuracy of mortality predictions is less dependent on the time horizon, and the relationship between the former and the latter is less pronounced. This could be explained by the relative stability of the number of mortality cases and the relatively static nature of (37).

Accuracy trajectories for the number of positive cases, inpatient, ICU and vent censuses are presented in Fig. 4. It can be observed that the most accurate predictions

[1] In general, our conclusions about the accuracy of the developed model, although arrived at through different means, are similar in nature to those reached in [23] with respect to the short-term forecasting model for Germany and Poland.

Variable	Positive cases			Inpatient census			ICU census			Vent census			Cumul. Mortality		
	Pred. 1 day ago	Pred. 1 wk. ago	Pred. 2 wks. ago	Pred. 1 day ago	Pred. 1 wk. ago	Pred. 2 wks. ago	Pred. 1 day ago	Pred. 1 wk. ago	Pred. 2 wks. ago	Pred. 1 day ago	Pred. 1 wk. ago	Pred. 2 wks. ago	Pred. 1 day ago	Pred. 1 wk. ago	Pred. 2 wks. ago
% correct	32%	27%	21%	38%	37%	29%	25%	31%	23%	20%	27%	28%	34%	33%	32%
med % err.	**0%**	**0%**	**1%**	**4%**	**6%**	18%	13%	11%	20%	18%	18%	24%	**1%**	**1%**	**2%**
av. % err.	2%	5%	16%	10%	15%	33%	21%	26%	40%	30%	39%	47%	2%	3%	3%
std. % err.	8%	29%	139%	14%	22%	95%	35%	55%	106%	47%	67%	89%	3%	3%	3%

Table 4. Accuracy of the NS COVID-19 model, Mar. 10, 2020 - May 24, 2021

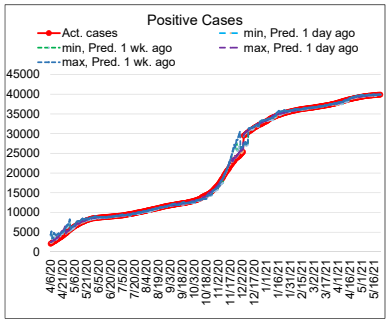

(a) Accuracy of the prediction for the number of NS cases

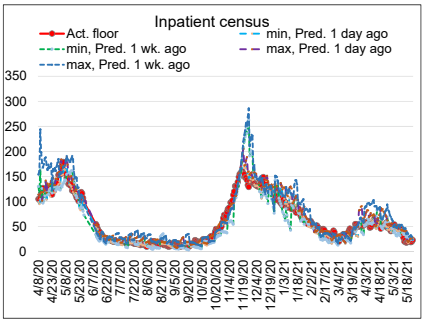

(b) Accuracy of the prediction for the floor census

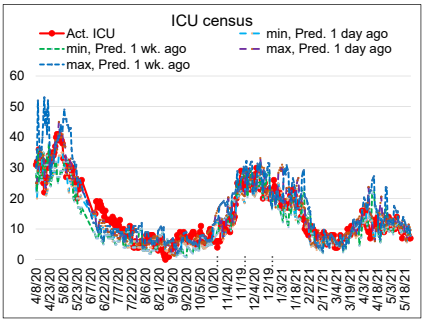

(c) Accuracy of the prediction for the ICU census

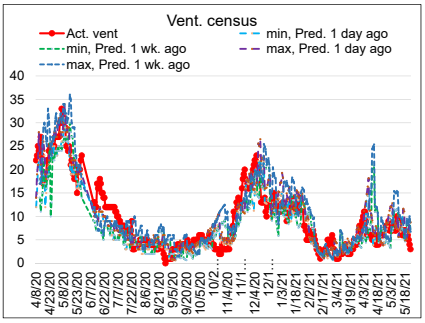

(d) Accuracy of the prediction for the vent census

Fig 4. Historical accuracy of predictions for the number of positive NS cases, floor, ICU and vent censuses, March 10, 2020 - May 24, 2021.

to date have been made during periods of relative "calm", i.e., those times when the infection curve followed a declining or quasi-static pattern (approximately, May - September 2020). Periods of elevated error include "regime changes" at the end of May 2020 and September 2020 to mid-January 2021. This was also to be expected given the uncertainty not captured by the moving average or polynomial extrapolation of the future transmission coefficient, R_0. Overall, the model appears to have "erred on the side of caution" overestimating the expected patient census while ICU and vent censuses tend to be underestimated more often, especially during the periods of "regime change".

Conclusion

The model provided acceptable predictive accuracy for the operational stakeholders to use it as an additional data point in their decision-making process. It was consistent with similar operational models adopted by healthcare and government entities in the region. While specifically designed for COVID-19, it could be repurposed for any communicable disease with high transmission, significant hospitalization, near zero reinfection and moderate mortality rates, provided sufficient requisite data describing its evolution in the community is available.

Acknowledgments

The authors would like to thank Emily Carter for thoroughly proofreading the manuscript and NorthShore University HealthSystem for the permission to use operational data in the publication of this research.

References

1. Kermack William Ogilvy and McKendrick A. G. A contribution to the mathematical theory of epidemics. Proc. R. Soc. Lond. A, 1927;115:700–721. https://royalsocietypublishing.org/doi/pdf/10.1098/rspa.1927.0118

2. Cooper I, Mondal A, Antonopoulos CG. A SIR model assumption for the spread of COVID-19 in different communities. Chaos, Solitons & Fractals. 2020;139:110057. doi:https://doi.org/10.1016/j.chaos.2020.110057.

3. Chen YC, Lu PE, Chang CS, Liu TH. A Time-Dependent SIR Model for COVID-19 With Undetectable Infected Persons. IEEE Transactions on Network Science and Engineering. 2020;7(4):3279–3294. doi:10.1109/tnse.2020.3024723.

4. Harko T, Lobo FSN, Mak MK. Exact analytical solutions of the Susceptible-Infected-Recovered (SIR) epidemic model and of the SIR model with equal death and birth rates. Applied Mathematics and Computation. 2014;236:184–194. doi:10.1016/j.amc.2014.03.030.

5. S SC, Selles MA PM, E PB. An Efficient COVID-19 Prediction Model Validated with the Cases of China, Italy and Spain: Total or Partial Lockdowns? J Clin Med. 2020; p. 1547. doi:10.3390/jcm9051547.

6. Konchak CW, Krive J, Au L, Chertok D, Dugad P, Granchalek G, et al. From Testing to Decision-Making: A Data-Driven Analytics COVID-19 Response. Academic Pathology. 2021;8:23742895211010257. doi:10.1177/23742895211010257.

7. Atkinson KE, Han W, Stewart D. Numerical Solution of Ordinary Differential Equations. John Wiley & Sons, Ltd; 2009. Available from: http://homepage.math.uiowa.edu/~atkinson/papers/NAODE_Book.pdf.

8. Ralston A. Runge-Kutta methods with minimum error bounds Math Comp. 1962; p. 431–437. doi:10.1090/S0025-5718-1962-0150954-0.

9. U.S. Census Bureau: Quick facts; 2019. https://factfinder.census.gov/faces/nav/jsf/pages/searchresults.xhtml?refresh=t.

10. Charles F. Manski and Francesca Molinari Estimating the COVID-19 infection rate: Anatomy of an inference problem. Journal of Econometrics. 2021, 220 (1), 181-192. doi:10.1016/j.jeconom.2020.04.041. https://www.sciencedirect.com/science/article/pii/S0304407620301676.

11. Ellen Brooks-Pollock, Leon Danon, Thibaut Jombart and Lorenzo Pellis Modelling that shaped the early COVID-19 pandemic response in the UK. UK. Philos Trans R Soc Lond B Biol Sci. 2021 Jul 19;376(1829):20210001. doi:10.1098/rstb.2021.0001

12. Jonathan M. Read, Jessica R. E. Bridgen, Derek A. T. Cummings, Antonia Ho and Chris P. Jewell Novel coronavirus 2019-nCoV (COVID-19): early estimation of epidemiological parameters and epidemic size estimates UK. Philos Trans R Soc Lond B Biol Sci. 2021 Jul 19;376(1829):20200265. doi:10.1098/rstb.2020.0265

13. Leon Danon, Ellen Brooks-Pollock, Mick Bailey and Matt Keeling A spatial model of COVID-19 transmission in England and Wales: early spread, peaktiming and the impact of seasonality UK. Philos Trans R Soc Lond B Biol Sci. 2021 Jul 19;376(1829):20200265. doi:10.1098/rstb.2020.0272

14. Paul Birrell, Joshua Blake, Edwin van Leeuwen, Nick Gent and Daniela De Angelis Real-time nowcasting and forecasting of COVID-19 dynamics in England: the first wave doi:10.1098/rstb.2020.0279

15. Thibaut Jombart, Stéphane Ghozzi, Dirk Schumacher, Timothy J. Taylor, Quentin J. Leclerc, Mark Jit, Stefan Flasche, Felix Greaves, Tom Ward, Rosalind M. Eggo, Emily Nightingale, Sophie Meakin, Oliver J. Brady, Centre for Mathematical Modelling of Infectious Diseases COVID-19 Working Group, Graham F. Medley, Michael Höhle and W. John Edmunds Real-time monitoring of COVID-19 dynamics using automated trend fitting and anomaly detection UK. Philos Trans R Soc Lond B Biol Sci. 2021 Jul 19;376(1829):20200266. doi:10.1098/rstb.2020.0266

16. Global convergence of COVID-19 basic reproduction number and estimation from early-time SIR dynamics PLoS One. 2020 Sep 24;15(9):e0239800 doi:10.1371/journal.pone.0239800

17. Nguemdjo U, Meno F, Dongfack A, Ventelou B. Simulating the progression of the COVID-19 disease in Cameroon using SIR models. PLoS One. 2020 Aug 25;15(8):e0237832. doi:10.1371/journal.pone.0237832

18. Calafiore GC, Novara C, Possieri C. A time-varying SIRD model for the COVID-19 contagion in Italy. Annu. Rev. Control. 2020;50:361-372. doi:doi: 10.1016/j.arcontrol.2020.10.005

19. Alanazi SA, Kamruzzaman MM, Alruwaili M, Alshammari N, Alqahtani SA, Karime A. Measuring and Preventing COVID-19 Using the SIR Model and Machine Learning in Smart Health Care. J. Healthc. Eng. 2020 Oct 29;2020:8857346. doi:10.1155/2020/8857346

20. Mandal M, Jana S, Khatua A, Kar TK. Modeling and control of COVID-19: A short-term forecasting in the context of India. Chaos. 2020 Nov;30(11):113119. doi:10.1063/5.0015330

21. Huang, Q., Mondal, A., Jiang, X., Horn, M. A., Fan, F., Fu, P., Wang, X., Zhao, H., Ndeffo-Mbah, M., Gurarie, D. SARS-CoV-2 transmission and control in a hospital setting: an individual-based modelling study. Royal Society open science, 2021, 8(3), 201895. doi:10.1098/rsos.201895

22. Bracher J, Ray EL, Gneiting T, Reich NG Evaluating epidemic forecasts in an interval format. PLOS Computational Biology 2021, 17(2): e1008618. doi:10.1371/journal.pcbi.1008618

23. J. Bracher, D. Wolffram, J. Deuschel, K. Görgen, J.L. Ketterer, A. Ullrich, S. Abbott, M.V. Barbarossa, D. Bertsimas, S. Bhatia, M. Bodych, N.I. Bosse, J.P. Burgard, L. Castro, G. Fairchild, J. Fuhrmann, S. Funk, K. Gogolewski, Q. Gu, S. Heyder, T. Hotz, Y. Kheifetz, H. Kirsten, T. Krueger, E. Krymova, M.L. Li, J.H. Meinke, I.J. Michaud, K. Niedzielewski, T. Ożański, F. Rakowski, M. Scholz, S. Soni, A. Srivastava, J. Zieliński, D. Zou, T. Gneiting, M. Schienle Short-term forecasting of COVID-19 in Germany and Poland during the second wave – a preregistered study, medRxiv 2020.12.24.2024882 doi:10.1101/2020.12.24.20248826

24. Tim K. Tsang, Peng Wu, Eric H. Y. Lau, Benjamin J. Cowling Accounting for imported cases in estimating the time-varying reproductive number of COVID-19 medRxiv 2021.02.09.21251416 doi:10.1101/2021.02.09.21251416

25. Jessica T. Davis, Matteo Chinazzi, Nicola Perra, Kunpeng Mu, Ana Pastore y Piontti, Marco Ajelli, Natalie E. Dean, Corrado Gioannini, Maria Litvinova, Stefano Merler, Luca Rossi, Kaiyuan Sun, Xinyue Xiong, M. Elizabeth Halloran, Ira M. Longini Jr., Cécile Viboud, Alessandro Vespignani Cryptic transmission of SARS-CoV-2 and the first COVID-19 wave in Europe and the United States medRxiv 2021.03.24.21254199 doi:10.1101/2021.03.24.21254199

26. Singh, B. B., Ward, M. P., Lowerison, M., Lewinson, R. T., Vallerand, I. A., Deardon, R., Gill, J., Singh, B., Barkema, H. W. Meta-analysis and adjusted estimation of COVID-19 case fatality risk in India and its association with the underlying comorbidities. One health (Amsterdam, Netherlands), 2021, 13. doi:10.1016/j.onehlt.2021.100283

27. Chiara Poletto, Samuel V Scarpino, Erik M Volz, Applications of predictive modelling early in the COVID-19 epidemic. The Lancet Digital Health, Volume 2, Issue 10, 2020, Pages e498-e499. doi:10.1016/S2589-7500(20)30196-5

28. Mattia Mazzoli, David Mateo, Alberto Hernando, Sandro Meloni, José J. Ramasco Effects of mobility and multi-seeding on the propagation of the COVID-19 in Spain medRxiv 2020.05.09.20096339 doi:10.1101/2020.05.09.20096339